



SPECTRAL ANALYSIS OF THE NUMERICAL VARIATION RESULT FOR ACOUSTIC CUT OFF FREQUENCY

P. Dileep Krishnan¹, Ramkumar Mishra²

Department of Physics

Maharishi University of Information Technology (U.P)

ABSTRACT

The thermal structure of the atmosphere of the Sun and other solar type stars has been one of the outstanding problems in solar physics and astrophysics for decades. The main aim of the paper is to perform the simulated numerically the behavior of acoustic waves in low layers of the solar atmosphere the upper photosphere and the lower and middle chromosphere, and use the spectral analysis of temporal wave profiles to calculate numerically variations of the acoustic cutoff frequency with height. The obtained numerical results are compared with the observational data. This variation may affect the acoustic cutoff period by 25% or less as compared to the case of constant γ , and will probably lead to a change of similar magnitude in the wave behavior in our numerical simulations. With good agreement between the theory and data, the results of this paper may become a basis for using the waves to determine the structure of the background solar atmosphere.

Key words: Acoustic cutoff frequency, solar atmosphere, hydrodynamics

1. INTRODUCTION

Propagation of acoustic waves in the solar atmosphere has been the subject of many analytical and numerical studies over several decades. The main goal of these studies has been to understand the transfer of wave energy from the solar convection zone, where the waves are generated, to the solar atmosphere, where they may dissipate their energy and heat the background atmosphere. The concept of acoustic cutoff frequency has played an important role in these studies, because it is this cutoff frequency that uniquely determines the propagation

conditions for acoustic waves in the solar atmosphere.

The acoustic cutoff (period) frequency was originally introduced by Lamb (1909, 1910), who first considered anisothermal atmosphere and showed that the resulting cutoff frequency is global (the same over the entire atmosphere) and is defined as the ratio of the sound speed to twice the scale height of pressure or density, these heights being the same. Lamb (1910, 1932) extended his studies of acoustic waves to an atmosphere with uniform temperature gradients and demonstrated how to define the acoustic cutoff in such a non-uniform medium. Lamb's work was followed by many others; specific applications related to solar physics were carried out by Moore & Spiegel (1964), Souffrin (1966), Summers (1976), Campos (1986), Fleck & Schmitz (1993), and more recently by Musielak et al. (2006), Fawzy & Musielak (2012), and Routh & Musielak (2014). Different expressions for the cutoff were derived analytically and used in different studies of acoustic waves in the solar atmosphere. However, a recent work by Wiśniewska et al. (2016) clearly demonstrated that these analytically obtained formulas failed to account properly for the observed variation of the cutoff with height in the solar atmosphere reported by these authors. The main goal of this paper is to perform numerical simulations of impulsively generated acoustic waves in the solar atmosphere, and use the spectral analysis of temporal wave profiles to calculate numerically variations of the acoustic cutoff frequency with height. The obtained numerical results are compared with the observational data. With good agreement between the theory and data, it is concluded that the results of this paper may become a basis for using the waves to determine

the structure of the background solar atmosphere.

2. MODEL OF THE SOLAR ATMOSPHERE

Our one-dimensional model of the solar atmosphere contains a gravitationally stratified and magnetic field-free plasma, which is described by the Euler equations with adiabatic index $\gamma=1.4$, gravity $\mathbf{g} = (0, -g, 0)$ with its solar value $g=274 \text{ m s}^{-2}$, and a mean particle mass m specified by a mean molecular weight 1.24. Our assumption of one-dimensionality can be justified because we consider acoustic waves propagating over the atmospheric height of 1 Mm. This height is comparable with the average size of a solar granule, which is taken to be a

source of the waves. As we aim to study a quiet solar region, we assume that initially, at time $t=10 \text{ s}$, low layers of the solar atmosphere are free of magnetic field and they are in static equilibrium (with velocity $V=10$) in which the equilibrium mass density and gas pressure are specified by a realistic, semi-empirical model of the plasma temperature $T(y)$ developed by Avrett & Loeser(2008). The atmospheric equilibrium described above is perturbed by a Gaussian pulse in the vertical, y -component of the velocity given by

$$V_y(y, t = 0) = A_v \exp\left[-\left(\frac{y - y_0}{w_y}\right)^2\right],$$

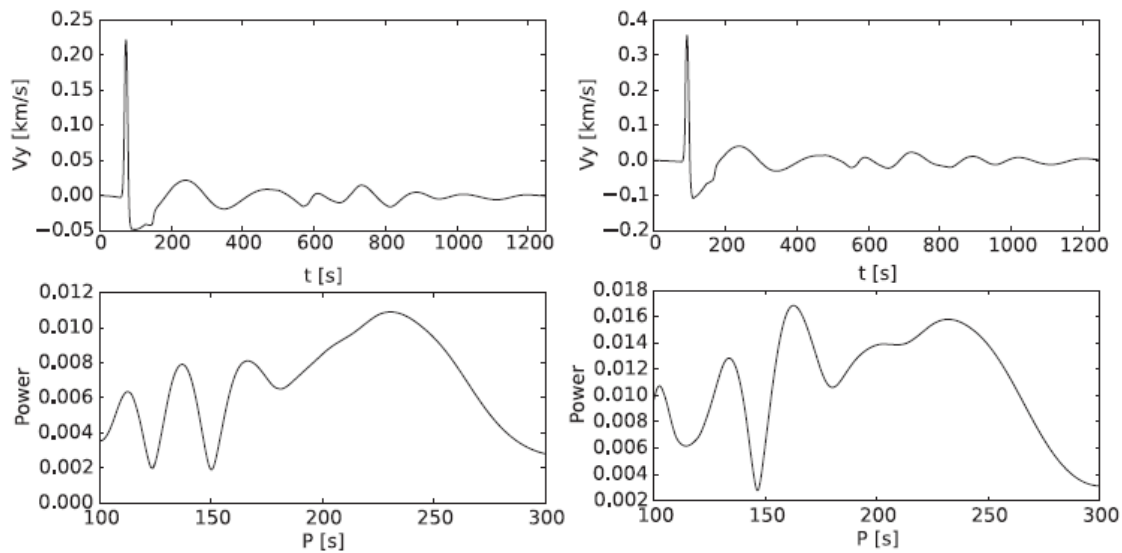


Figure 1. Time signatures (top panels) and their periodograms (bottom panels)

Where y is the vertical coordinate, A_v is the amplitude of the pulse, y_0 is its initial position, and $w_y=50 \text{ km}$ denotes its width along the vertical direction. This initial pulse corresponds to a packet of waves with its Gaussian spectrum characterized by wavenumber k . Since locally a different k corresponds to a different cyclic frequency ω , we actually have a packet of waves with different ω . Once this packet propagates through the solar atmosphere, the atmosphere filters those wave frequencies that correspond to propagating acoustic waves; waves that become evanescent do not appear at greater atmospheric heights. It is this very characteristic behavior of the waves that is considered here to determine variations of the acoustic cutoff with height, and compare the numerically obtained wave periods to

the observational data reported by Wiśniewska et al. (2016).

3. NUMERICAL RESULTS

We solve the equations of hydrodynamics numerically by using the PLUTO code, in which we adopted the HLLD Riemann solver and min mod flux-limiter (Mignone et al. 2012). Numerical simulations are performed in the model of the solar atmosphere described in Section 2. The simulation region is set as $-0.5 < y < 40 \text{ Mm}$. At the bottom and top boundaries we set all plasma quantities to their equilibrium values. The region $-0.5 < y < 6.68 \text{ Mm}$ is covered by 1536 uniform grid points, while the top level is represented by 512 numerical cells that grow in size with height. Such a stretched grid works as a sponge, absorbing the

incoming signal, and it results in negligibly small wave reflection from the top boundary. This very long domain and the boundary type are not relevant for this simulation, because although the

waves reach the upper boundary within the time range of interest they are strongly diffused in the top region, and therefore they do not affect the wave behavior below the transition region.

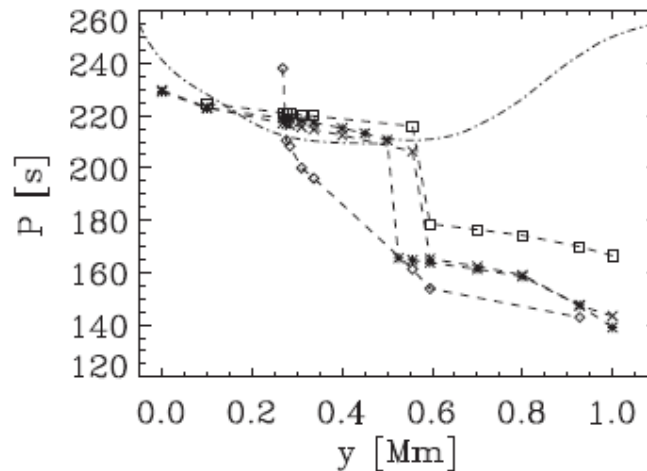


Figure 2. The dominant wave periods vs. height y for $A_v = 0.1 \text{ km s}^{-1}$ and $y_0 = -150 \text{ km}$

As a result of the initial pulse given by Equation (1), acoustic waves are generated (Figure 1, top panels) and they propagate in the model of the solar atmosphere. As shown first by Lamb (1909), the presence of gravity leads to the appearance of the acoustic cutoff period, $P_{ac} = 4pL / cs$, where ΔT is the pressure scale height, which becomes responsible for the propagation of the waves if their period P is smaller than P_{ac} , or their evanescence if P becomes comparable to or larger than P_{ac} . It must be noted that in the realistic solar atmosphere considered here, P_{ac} is a local quantity (e.g., Musielak et al. 2006; Routh & Musielak 2014) that varies significantly with height. Lamb (1909, 1932) also showed that an initial pulse results in a wave front that propagates away from the launching region. The wave front is followed by an oscillating wake, which oscillates at the wave period P_{ac} and whose amplitude declines in time. We analyze the time signal of $V_y(y, t)$ that is collected at two altitudes: $y=0.4$ and 0.525 Mm (Figure 1). The leading wave front and oscillating wake are clearly seen in the time signatures (top panels). These time signatures are analyzed spectrally to obtain power spectra (Figure 1, bottom panels) that allow us to determine the dominant wave period P for each detection point. Note that for $y=0.4 \text{ Mm}$ the maximum of $P \approx 220 \text{ s}$ is followed by a smaller local maximum at $P \approx 170 \text{ s}$. For $y=0.525 \text{ Mm}$; the second local maximum has

already become the dominant wave period, while the former maximum at $P \approx 220 \text{ s}$ is now a local maximum. This simply means that at $y=0.4 \text{ Mm}$ most of the wave energy is associated with waves of longer period, but just above this, mainly at $y=0.525 \text{ Mm}$, waves of shorter period become dominant.

Figure 2 illustrates the numerically evaluated dominant wave period, P , which is plotted versus altitude y ; the observational data of Wiśniewska et al. (2016) are represented by diamonds, and the acoustic cutoff wave period, P_{ac} , as a dashed-dotted line. Note that the data for case (a) are closest to the observational findings (diamonds). Intuitively, we expect that an initial pulse of larger amplitude should result in longer wave periods. Indeed, Figure 2 confirms that. For more deeply launched pulses, such as in case (c), a larger-amplitude oscillating tail is seen, and P in case (c) is larger than P in case (a). Moreover, for low values of y the dominant wave periods are shorter than P_{ac} , and the acoustic waves propagate in these atmospheric layers. However, for $y > 0.15 \text{ Mm}$ we find that $P > P_{ac}$, and as a result, the acoustic waves become evanescent. The long dominant wave period seen in Figure 1 reduces its magnitude and the lagging first local maximum in P becomes dominant for $y=0.525 \text{ Mm}$; this means that much of the energy carried by the waves has been converted into short-period waves. As $P < P_{ac}$ for $y > 0.55 \text{ Mm}$, the

acoustic waves of such periods are propagating in the atmosphere. Note that values of P are within the range of about 140–240 s, which corresponds to oscillations of approximately 2.5–4 minutes. The numerically detected wave periods exhibit a fall-off with height for all chosen parameters and the numerical results are close to the observational data reported by Wiśniewska et al. (2016).

4. CONCLUSIONS

In this paper, we simulated numerically the behavior of acoustic waves in low layers of the solar atmosphere that are free of magnetic field and invariant along horizontal directions. Our main goal was to reconcile theory with the most recent observations performed by Wiśniewska et al. (2016), who demonstrated how the acoustic cutoff varies with height in the solar atmosphere. In our approach, the waves are excited by a single initial pulse in the vertical component of velocity with amplitude $A_v=0.1$ km s⁻¹ or $A_v=0.25$ km s⁻¹, and the pulse leads to a spectrum of acoustic waves of different periods that propagate throughout the background solar atmosphere. During this propagation, the spectrum is filtered by the atmosphere, and we used its non-propagating part representing standing acoustic waves to determine the resulting acoustic cutoff period, which varies with height. The numerically obtained decreasing trend of the dominant wave period generally matches the observational data of Wiśniewska et al. (2016). The agreement clearly indicates that the obtained numerical results may be used as a basis to determine the structure of the background solar atmosphere. Finally, we want to point out that all presented results were obtained with fixed $\gamma=1.4$ and that the OPAL equation of state would lead to the adiabatic index in the solar atmosphere varying between 1.1 and 1.66 within the first 1.5Mm above the solar surface. This variation may affect the acoustic cutoff period by 20% or less as compared to the case of constant γ , and will probably lead to a change of similar magnitude in the wave behavior in our numerical simulations.

REFERENCES

- [1] Avrett, E. H., & Loeser, R. 2008, ApJS, 175, 229
- [2] Campos, L. M. B. C. 1986, RvMP, 58, 117
- [3] Carlsson, M., & Stein, R. F. 1997, ApJ, 481, 500
- [4] Cuntz, M., Ulmschneider, P., & Musielak, Z. E. 1998, ApJL, 493, L117
- [5] Fawzy, D. E., & Musielak, Z. E. 2012, MNRAS, 421, 159
- [6] Fawzy, D. E., Rammacher, W., Ulmschneider, P., Musielak, Z. E., &
- [7] Stępień, K. 2002, A&A, 386, 971
- [8] Fleck, B., & Schmitz, F. 1993, A&A, 273, 487
- [9] Jiménez, A. 2006, ApJ, 646, 1398
- [10] Jiménez, A., García, R. A., & Pallé, P. L. 2011, ApJ, 743, 99
- [11] Lamb, H. 1909, Proc. London Math. Soc., 7, 122
- [12] Lamb, H. 1910, RSPSA, 34, 551
- [13] Lamb, H. 1932, Hydrodynamics (New York: Dover)
- [14] Mignone, A., Zanni, C., Tzeferacos, P., et al. 2012, ApJS, 198, 31
- [15] Moore, D. W., & Spiegel, E. A. 1964, ApJ, 139, 48
- [16] Musielak, Z. E., Musielak, D. E., & Mobashi, H. 2006, PhRvE, 73, 036612
- [17] Routh, S., & Musielak, Z. E. 2014, AN, 335, 1043
- [18] Souffrin, P. 1966, AnAp, 39, 55
- [19] Summers, D. 1976, QJMAM, 29, 117
- [20] Ulmschneider, P. 1971, A&A, 14, 275
- [21] Ulmschneider, P., Schmitz, F., Kalkofen, W., & Bohn, H. U. 1978, A&A, 70, 487
- [22] Wiśniewska, A., Musielak, Z. E., Staiger, J., & Roth, M. 2016, ApJL, 819, L23